

# A brilliant sandwich type fluorescent nanostructure incorporating a compact quantum dot layer and versatile silica substrates†

Cite this: *Chem. Commun.*, 2014, 50, 2896

Received 2nd November 2013,  
Accepted 18th December 2013

Liang Huang, Qiong Wu, Jing Wang, Mohamed Foda, Jiawei Liu, Kai Cai and Heyou Han\*

DOI: 10.1039/c3cc48405j

www.rsc.org/chemcomm

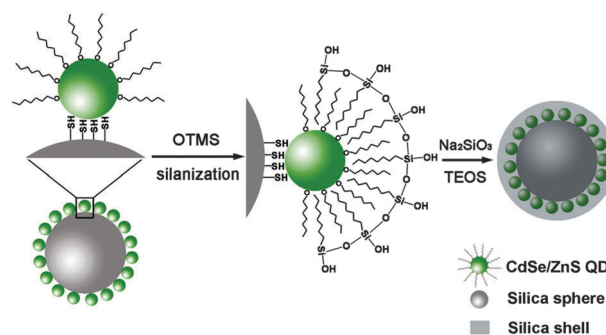
**A “hydrophobic layer in silica” structure was designed to integrate a compact quantum dot (QD) layer with high quantum yield into scalable silica hosts containing desired functionality. This was based on metal affinity driven assembly of hydrophobic QDs with versatile silica substrates and homogeneous encapsulation of organosilica/silica layers.**

Assembling hydrophobic nano-building blocks directly with solid or colloidal substrates in an organic phase<sup>1,2</sup> brings a new opportunity to achieve high particle packing density, exceeding the limitation of aqueous-based layer-by-layer self assembly where electrostatic repulsion among similarly charged particles exists.<sup>3,4</sup> For semiconductor nanocrystals, namely quantum dots (QDs), skipping the conventional hydrophilic ligand exchange<sup>5</sup> before assembly particularly favors their surface passivation to maintain bright and sharp emissions. These characteristics make such assembly technically attractive for fabricating high performance QD based fluorescent structures which have broad applications in multiplex analysis by color encoding,<sup>6</sup> simultaneously visualizing intracellular targets<sup>7</sup> and ultrasensitive fluorescent imaging.<sup>8</sup>

The primary concern in structural engineering of such hydrophobic QD assemblies is to achieve high fluorescence, multi-functionality and bio-compatibility. Unfortunately, the fluorescent sensitivity of QDs towards native organic ligand passivation makes their processing a challenging issue, due to an irreversible quantum yield (QY) loss. This occurred in either assembly process requires pre-modification of the QD surface<sup>9–11</sup> or post-grafting of an immobilized QD layer with hydrophilic coatings.<sup>8</sup> Despite using multilayer-shell passivation could render QDs less sensitive to surface damage,<sup>8,12,13</sup> yet the synthetic protocol is rather complicated compared with that of generally available QDs (CdSe/ZnS in most cases). In that sense, exploring a “minimally invasive” incorporation of an intact QD layer into processable substrates would benefit the fluorescent nanostructure design.

Silica is one superior candidate as both a supporting substrate and hydrophilic coating layer due to its convenient processability, high stability in aqueous media and good biocompatibility.<sup>14,15</sup> The strong coordination of thiolated silica with metal containing nanoparticles<sup>2b</sup> may serve efficiently in achieving high QY and simplified protocols, since no pre-modification for hydrophobic QDs is required. On the other hand, the combination of a hydrophobic bilayer with a silica shell<sup>16</sup> would largely preserve both the QY and the QD loading amount to give bright and stable water dispersible QD structures. Surfactant encapsulation has been adopted to mediate the phase transfer of hydrophobic particle assemblies,<sup>2b</sup> this may promote a subsequent mesoporous silica shell<sup>17</sup> instead of a homogeneous coating due to the aggregation of silica together with surfactant micelles.<sup>18</sup>

Herein, a QD based fluorescent nanostructure simultaneously possessing a high QY and homogeneous silica coating was prepared, using a silica anchoring surface and an alkyl-chain derived organosilica shell to sandwich a compact layer of hydrophobic QDs. As shown in Scheme 1, the QDs were efficiently immobilized by SiO<sub>2</sub> substrates *via* thiol–metal coordination to achieve a high loading. The hydrophobic assemblies underwent an ultrasonic assisted silanization by *n*-octyl trimethoxy silane (OTMS) to derive an amphiphilic organosilica layer, which was critical to achieving a high QY and a homogeneous silica coating



**Scheme 1** Preparation procedure of sandwich type SiO<sub>2</sub>@QDs@SiO<sub>2</sub> fluorescent nanostructure.

State Key Laboratory of Agricultural Microbiology, College of Science, Huazhong Agricultural University, Wuhan 430070, China.

E-mail: hyhan@mail.hzau.edu.cn; Fax: +86-27-87288246; Tel: +86-27-87288246

† Electronic supplementary information (ESI) available: Experimental details and supporting figures. See DOI: 10.1039/c3cc48405j

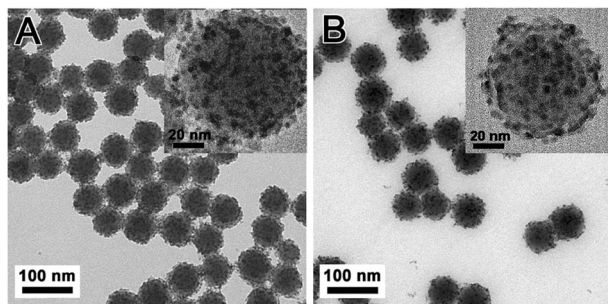


Fig. 1 TEM images of  $\text{SiO}_2$ @QDs assemblies in organic phase (A) and  $\text{SiO}_2$ @QDs@ $\text{SiO}_2$  spheres in water (B). Insets are enlarged images of a single sphere.

from silicate deposition and desired Stöber growth. The current assembly and coating strategy was further extended to fabricate variably sized and bi-functional fluorescent nanostructures.

Colloidal silica substrates were first grafted with mercaptopropyl groups for anchoring with QD surface metals. The thiolated spheres exhibited good monodispersity (Fig. S1A, ESI<sup>†</sup>) and enhanced hydrophobicity to disperse in nonpolar solvents, which favored their proper interaction with CdSe/ZnS QDs (Fig. S1B, ESI<sup>†</sup>). The highly efficient thiol–metal coordination driven assembly produced surface saturated silica spheres by QDs (Fig. 1A) which rendered them totally dispersible in an organic phase. To confirm the driving force of the QD assembly with a thiolated surface, the QDs were preliminarily incubated with dodecanethiol (DDT) which could hinder further ligand exchange of the QDs after its strong coordination to metals.<sup>12,19</sup> As illustrated in Fig. S2A (ESI<sup>†</sup>), when a small amount of DDT was introduced before the assembling, a significantly decreased amount of QDs on the silica spheres was visualized, accompanied by aggregation of the spheres due to reduced surface hydrophobicity in toluene. With excess DDT addition, only limited QDs were captured by silica spheres and severe aggregation occurred (Fig. S2B, ESI<sup>†</sup>). This hindering effect on the QDs immobilization efficiency by alkanethiol primarily supports partial exchange of original QD ligands by thiol groups on the colloidal silica surface during assembly.

To achieve a homogeneous silica coating on hydrophobic particles, a vitreophilic surface is required. The hydrophobic  $\text{SiO}_2$ @QDs assemblies were dissolved in OTMS and dispersed in methanol to form a homogeneous colloidal solution with the aid of ultrasonication. Ammonia (2.5 vol%) was employed to catalyze the hydrolysis of the siloxane moieties from OTMS forming amphiphilic silanetriols which rendered the  $\text{SiO}_2$ @QDs assemblies water soluble. At the initial stage, the partially hydrolyzed organosilane was visualized as a corona surrounding the assemblies which were easy to coalesce (Fig. S3A, ESI<sup>†</sup>). With sufficient hydrolysis of OTMS, the organosilane encapsulated spheres showed a relatively smooth surface with improved particle dispersity in water (Fig. S3B, ESI<sup>†</sup>). The complexity of QD assemblies compared with individual QDs in silanization involves the possible desorption of QDs if any intense phase dispersion occurs. In this context, performing ultrasonic dispersion in the homogeneous phase (OTMS in alcohol) was critical for the  $\text{SiO}_2$ @QDs assemblies to maintain a high QD loading amount. Conversely, dispersing the silane precursor directly into

water as we previously adopted to silanize pure QDs<sup>16c</sup> induced a severe desorption of QDs from the silica surface (Fig. S3C, ESI<sup>†</sup>). This was probably caused by the breaking of existing thiol–metal coordination during the severe fragmentation of the OTMS emulsion droplet (by cavitation), since the OTMS and QD assemblies formed a dispersion phase in water.

To achieve well controlled silica growth around the host, the Stöber process was frequently adopted. Before this step, the particles were pre-coated with a thin layer of active silica to prevent flocculation in low polar solvents for reduced electrostatic repulsion.<sup>20</sup> As demonstrated in Fig. 1B, the  $\text{SiO}_2$ @QDs assemblies after silicate deposition maintained the same morphology as in an oil phase, while the featureless silica coating layer could be hardly identified under TEM. We suspect this originated from the oligomeric nature of the active silica formed in aqueous solution.<sup>20</sup> Nevertheless, this silicate deposition procedure has a crucial role in stabilizing the  $\text{SiO}_2$ @QDs assemblies in the Stöber system even after a deposition time of 12 h, while the assemblies right after organosilica coating appeared partially flocculated in a water–alcohol mixture.

Unlike the irreversible photoluminescence (PL) quenching of QDs upon ligand exchange based silica coating strategies, we observed a well retained PL emission using an organosilica/silica bilayer coating. As shown in Fig. S4 (ESI<sup>†</sup>), after a temporary PL degradation in the phase transfer process, the PL intensity increased almost one-fold after 12 h active silica growth. This PL recovery behavior was probably favored by the accomplishment of silanol condensation and silica shell growth around the QDs which effectively isolated them from the external aqueous environment.<sup>16b,c</sup> To determine the QY, the  $\text{SiO}_2$ @QDs@ $\text{SiO}_2$  spheres were dispersed in an ethanol–toluene mixture which has a reflective index approaching that of silica to minimize the light scattering effect.<sup>11</sup> In this manner, the QY of the fluorescent spheres was measured as 42% (84% normalized to hydrophobic QDs with a QY of 50%). The absorption and PL spectra of the QDs after assembly and silica coating also maintained the same profiles as in an oil phase, as depicted in Fig. 2A. Time-resolved photoluminescence was performed to verify this PL preservation. The PL decay curve of the  $\text{SiO}_2$ @QDs@ $\text{SiO}_2$  spheres was almost identical to the oil soluble QDs (Fig. 2B) with tiny changes in fitting parameters (Table S1, ESI<sup>†</sup>). These results

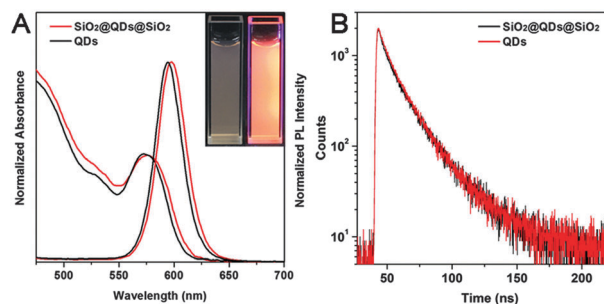


Fig. 2 (A) UV-vis absorption and PL spectra of oil soluble QDs and  $\text{SiO}_2$ @QDs@ $\text{SiO}_2$  fluorescent spheres (inset: photographs of fluorescent spheres in aqueous solution under a visible light and a UV lamp). (B) PL decay curves of  $\text{SiO}_2$ @QDs@ $\text{SiO}_2$  fluorescent spheres and oil soluble QDs.

evidently indicated a good retention in QD emission character using an organosilica interlayer to preserve the original ligands of the QDs.

Due to the formation of stable dispersions in the Stöber system, a thicker silica shell could be deposited on the assemblies desirably. Fig. S5 (ESI<sup>†</sup>) illustrates the morphology of the SiO<sub>2</sub>@QDs@SiO<sub>2</sub> spheres at different coating stages in the Stöber process. At the beginning, the silica grew preferentially around the QD surface (Fig. S5A, ESI<sup>†</sup>), indicating the localization of silanol anchor points on individual QDs. Subsequently, the small silica particles containing single QDs began to merge with each other forming an intact silica layer (Fig. S5B and C, ESI<sup>†</sup>). The silica shell displayed a relatively smooth surface at a thickness of 30 nm and the QDs layer on the original silica substrates could be resolved as a dark and compact ring (Fig. S5D, ESI<sup>†</sup>).

The unique processability of colloidal silica enables facile tailoring and functionalization of the inner substrates. Here we demonstrate the scaling of fluorescent nanosphere size using 93 nm and 200 nm silica substrates. After the assembling and coating procedures, the SiO<sub>2</sub>@QDs@SiO<sub>2</sub> fluorescent spheres with uniform size and compact QD loading were obtained (Fig. 3A–D). This strategy also allows the design of bi-functional materials from both the interior and exterior of colloidal silica substrates.

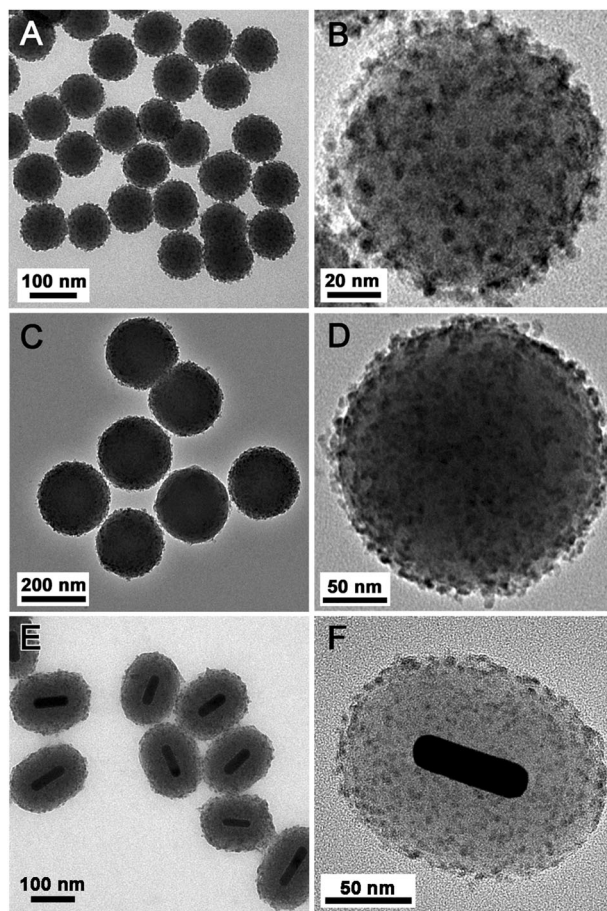


Fig. 3 TEM images of SiO<sub>2</sub>@QDs@SiO<sub>2</sub> fluorescent spheres with 93 nm (A, B) and 200 nm (C, D) SiO<sub>2</sub> substrates and AuNR@SiO<sub>2</sub>@QDs@SiO<sub>2</sub> bi-functional nanocomposites (E, F).

As illustrated in Fig. 3E and F, the QD layers were successfully incorporated into gold nanorod (AuNR) embedded silica substrates with high loading densities. The good dispersity of such composite nanostructures in the aqueous phase indicated the successful encapsulation of the outer silica layer. Encouragingly, the prepared AuNR@SiO<sub>2</sub>@QDs@SiO<sub>2</sub> nanocomposites exhibited both the original near infrared absorption feature of the AuNRs and the intrinsic fluorescence of the CdSe/ZnS QDs (Fig. S6, ESI<sup>†</sup>), indicating their potential as multimodal imaging and theranostic agents.

In summary, a versatile sandwich type silica nanostructure integrated with a highly fluorescent QD layer was developed. The inner silica substrates with high uniformity, scalable size and functional contents were immobilized with a compact hydrophobic QDs layer exhibiting a bright and sharp emission, which were encapsulated by an organosilica and silica shell to maintain the compact loading and high fluorescence. The surfactant free silanization by lipophilic silane was critical to achieving a high QY and a homogeneous silica coating around the QD assemblies. This strategy enables us to make full use of high quality nanoparticle building blocks from the organic phase to build bio-compatible nanostructures with amplified signals and multi-functionality.

This work is supported by National Natural Science Foundation of China (21175051, 21375043) and the Natural Science Foundation of Hubei Province Innovation Team (2011CDA115).

## Notes and references

- (a) Y. Kim, C. Lee, I. Shim, D. Wang and J. Cho, *Adv. Mater.*, 2010, **22**, 5140; (b) Y. Ko, H. Baek, Y. Kim, M. Yoon and J. Cho, *ACS Nano*, 2012, **7**, 143.
- (a) Z. Lu, J. Goebl, J. Ge and Y. Yin, *J. Mater. Chem.*, 2009, **19**, 4597; (b) Z. Lu, C. Gao, Q. Zhang, M. Chi, J. Y. Howe and Y. Yin, *Nano Lett.*, 2011, **11**, 3404.
- K. C. Grabar, P. C. Smith, M. D. Musick, J. A. Davis, D. G. Walter, M. A. Jackson, A. P. Guthrie and M. J. Natan, *J. Am. Chem. Soc.*, 1996, **118**, 1148.
- J. Schmitt, G. Decher, W. J. Dressick, S. L. Brandow, R. E. Geer, R. Shashidhar and J. M. Calvert, *Adv. Mater.*, 1997, **9**, 61.
- (a) M. Bruchez, M. Moronne, P. Gin, S. Weiss and A. P. Alivisatos, *Science*, 1998, **281**, 2013; (b) W. C. Chan and S. Nie, *Science*, 1998, **281**, 2016; (c) H. Mattoussi, J. M. Mauro, E. R. Goldman, G. P. Anderson, V. C. Sundar, F. V. Mikulec and M. G. Bawendi, *J. Am. Chem. Soc.*, 2000, **122**, 12142.
- (a) M. Han, X. Gao, J. Z. Su and S. Nie, *Nat. Biotechnol.*, 2001, **19**, 631; (b) P. S. Eastman, W. M. Ruan, M. Doctolero, R. Nuttall, G. de Feo, J. S. Park, J. S. Chu, P. Cooke, J. W. Gray, S. Li and F. F. Chen, *Nano Lett.*, 2006, **6**, 1059.
- L. L. del Mercato, A. Z. Abbasi, M. Ochs and W. J. Parak, *ACS Nano*, 2011, **5**, 9668.
- B. H. Jun, D. W. Hwang, H. S. Jung, J. Jang, H. Kim, H. Kang, T. Kang, S. Kyeong, H. Lee and D. H. Jeong, *Adv. Funct. Mater.*, 2012, **22**, 1843.
- B. Lee, Y. Kim, S. Lee, Y. S. Kim, D. Wang and J. Cho, *Angew. Chem., Int. Ed.*, 2010, **49**, 359.
- M. Yoon, Y. Kim and J. Cho, *ACS Nano*, 2011, **5**, 5417.
- Y. Chan, J. P. Zimmer, M. Stroh, J. S. Steckel, R. K. Jain and M. G. Bawendi, *Adv. Mater.*, 2004, **16**, 2092.
- R. Kooles, M. M. van Schooneveld, J. Hilhorst, C. de Mello Donegá, D. C. Hart, A. van Blaaderen, D. Vanmaekelbergh and A. Meijerink, *Chem. Mater.*, 2008, **20**, 2503.
- Z. Popović, W. Liu, V. P. Chauhan, J. Lee, C. Wong, A. B. Greytak, N. Insin, D. G. Nocera, D. Fukumura and R. K. Jain, *Angew. Chem., Int. Ed.*, 2010, **122**, 8831.
- (a) Y. Piao, A. Burns, J. Kim, U. Wiesner and T. Hyeon, *Adv. Funct. Mater.*, 2008, **18**, 3745; (b) A. Guerrero-Martínez, J. Pérez-Juste and L. M. Liz-Marzán, *Adv. Mater.*, 2010, **22**, 1182.

- 15 M. A. Malvindi, V. Brunetti, G. Vecchio, A. Galeone, R. Cingolani and P. P. Pompa, *Nanoscale*, 2012, **4**, 486.
- 16 (a) Z. Zhelev, H. Ohba and R. Bakalova, *J. Am. Chem. Soc.*, 2006, **128**, 6324; (b) R. Han, M. Yu, Q. Zheng, L. Wang, Y. Hong and Y. Sha, *Langmuir*, 2009, **25**, 12250; (c) L. Huang, Z. Luo and H. Han, *Chem. Commun.*, 2012, **48**, 6145.
- 17 (a) I. Gorelikov and N. Matsuura, *Nano Lett.*, 2008, **8**, 369; (b) J. Kim, H. S. Kim, N. Lee, T. Kim, H. Kim, T. Yu, I. C. Song, W. K. Moon and T. Hyeon, *Angew. Chem., Int. Ed.*, 2008, **47**, 8438; (c) X. Hu, P. Zrazhevskiy and X. Gao, *Ann. Biomed. Eng.*, 2009, **37**, 1960.
- 18 R. I. Nooney, D. Thirunavukkarasu, Y. Chen, R. Josephs and A. E. Ostafin, *Chem. Mater.*, 2002, **14**, 4721.
- 19 R. Xie, M. Rutherford and X. Peng, *J. Am. Chem. Soc.*, 2009, **131**, 5691.
- 20 L. M. Liz-Marzán, M. Giersig and P. Mulvaney, *Langmuir*, 1996, **12**, 4329.